

# Emission of photoelectrons and their impact on the plasma sheath in hydrogen plasmas

D. Wunderlich, U. Fantz and the NNBI team

*Max-Planck-Institut für Plasmaphysik, Boltzmannstr. 2, 85748 Garching, Germany*

The interaction of UV photons with low work function surfaces can lead to an intense emission of photoelectrons. In plasmas these photo electrons can modify the properties of the plasma sheath and the bulk plasma close to the surface. This effect can be of particular relevance when in a tandem-type plasma source intense UV radiation is created in the hot and dense part of the plasma and then interacts with low work function surfaces in the cold and thin part. One example for tandem-type sources is the prototype negative hydrogen ion source for ITER NBI. In order to determine the UV photon fluxes in this source, ro-vibrationally resolved corona models for different transitions in the H<sub>2</sub> molecule have been developed. In combination with appropriate quantum efficiencies and a particle-in-cell code the amount of photo electrons emitted at the surfaces and their impact on the plasma properties is determined: the flux of photo electrons is by a factor of about 157 smaller than the production rate of surface produced negative hydrogen ions. Due to the small flux and mass of the photoelectrons, their effect on the plasma sheath, the bulk plasma and the negative ion flux towards the bulk plasma is negligible.

## 1. Introduction

UV photons impinging a low work function surface lead to the production of photoelectrons (PE). The number of PE produced per incident photon is described by an energy and material-dependent conversion factor, the so-called quantum efficiency (QE). In plasmas, the additional space charge caused by the PE can modify the shape of the plasma sheath and consequently also the properties of the bulk plasma. This effect is expected to be particularly pronounced in tandem-type plasma sources when an intense flux of UV photons created in the hot and dense part of the plasma interacts with surfaces in the cold and thin part of the plasma.

A typical tandem-type plasma source is the prototype negative hydrogen ion source[1] for ITER neutral beam injection (NBI). The UV photons are produced predominately in the so-called driver. A strong production of PE is expected at the surface of the plasma grid (PG, the first grid of the extraction system) since the work function of this surface is low (due to coverage with a thin layer of caesium; its purpose is to enhance the surface production [2] of negative hydrogen ions). In a previous publication [3] the amount of UV photons impinging the PG was estimated by calculations with a vibrationally resolved collisional radiative (CR) model. Using the QE for caesiated tungsten surfaces[4] the resulting PE flux was determined. Finally, this PE flux was used as input for the 1d3v particle-in-cell (PIC) code `Bacon`[5] in order to determine the shape of the plasma sheath and the properties of the bulk plasma. The predicted

influence of the PE on the plasma sheath and the bulk plasma was very small.

However, these previous investigations considered only one emission band of H<sub>2</sub> generating UV photons, namely the continuum  $a^3 \rightarrow b^3$  (most intense part between 150 nm ÷ 350 nm). Other bands producing significant amounts of UV photons have been neglected, the most relevant ones are the Werner band  $C^1 \rightarrow X^1$  ( $\lambda=90$  nm ÷ 130 nm) and the Lyman band  $B^1 \rightarrow X^1$  ( $\lambda=130$  nm ÷ 165 nm). Additionally, for the previous calculations a too high QE was implemented by mistake into the PIC code, resulting in a too high PE flux generated at the converter surface. By including the Werner and Lyman bands to the calculations the amount of UV photons will increase and by correcting the used QE, the amount of PE will decrease. The combined effect of both modifications cannot be estimated in a simple way.

In order to determine the amount of UV photons generated by the Werner and Lyman bands new ro-vibrationally resolved corona models for these transitions have been developed. The two models and their application to the prototype negative ion source for ITER NBI – in combination with the existing CR model for the  $a^3 \rightarrow b^3$  transition – are described in the following.

## 2. Population models for H<sub>2</sub>

The population density  $n_p$  of an excited state  $p$  in H<sub>2</sub> – and hence also the amount of photons emitted by spontaneous emission from this state – is correlated to different (depending on the plasma

regime) plasma parameters (e.g. the electron temperature  $T_e$ , the electron density  $n_e$ , the ground state densities of H and  $H_2$ , the gas temperature, the particle densities of the different ionic species and the respective temperatures).

Thus, necessary for predicting the amount of emitted UV photons emitted by molecular transitions in hydrogen plasmas are population models for  $H_2$ . These models use as input the plasma parameters and calculate for all excited states  $p$  implemented to the model  $n_p$ . Low-pressure, low-temperature plasmas are described best by corona models or CR models. Such models can be used either for backward or for forward calculations. The prior application allows – in combination with measured population densities (e.g. determined by optical emission spectroscopy) – determining plasma parameters by varying the respective input parameters of the model until the simulated spectrum best matches the measured spectrum. Forward calculations allow for known plasma parameters predicting the amount of photons emitted in a certain wavelength range.

While well benchmarked CR models for the hydrogen atom are available for a couple of years now [6,7,8] the situation for  $H_2$  is completely different: for detailed investigations of the  $H_2$  emission bands a population model should be applied that takes into account the electronically, vibrationally and rotationally excited states of  $H_2$ . Such a model does not exist up to now. Most models for  $H_2$  take into account only the electronic states, a few models (e.g. the one used in [3]) consider also some or all of the vibrational states. The corona models for the Werner and Lyman bands of  $H_2$  introduced by this presentation are first steps towards a ro-vibrationally resolved CR model for  $H_2$ .

### 3. Simulating $H_2$ emission bands

#### 3.1. Collisional radiative modelling of $H_2$

Corona models and CR models solve rate equations which balance populating and depopulating reaction channels for each excited state of an atom or molecule. Corona models take into account only electron collision excitation from the ground state and de-excitation by spontaneous emission. CR models consider a much larger amount of reaction channels, including stepwise excitation and excitation by cascades from energetically higher levels. As a consequence, corona models can be applied only for plasmas with a very low  $n_e$  ( $<10^{17} \text{ m}^{-3}$ ) while CR models are applicable in a much broader parameter range. In corona models the

rate equations for all states are decoupled from each other; in CR models the equations form a system of coupled ordinary differential equations. Within the scope of this work the flexible solver *Yacora* [6] is used for solving the equation system.

Figure 1 shows the lowest electronic states of  $H_2$ . Due to two different possible combinations of the electron spins, a singlet and a triplet system are present. Transitions between these systems are optically forbidden and are only possible by electron exchanging collision processes. For each of the electronic states additionally vibrational and rotational excitation is possible. The resulting number of electronically, vibrationally and rotationally excited states is very large. Consequently, also the number of reactions for which probabilities (mainly transition probabilities for spontaneous emission and electron collision excitation cross sections) are needed as input is high. Even for the hydrogen molecule – the simplest existing molecule – the existing data base is by far not complete: a full set of vibrationally resolved transition probabilities exists [9] and for some transitions ro-vibrationally resolved transition probabilities are available [10,11]. Most excitation cross sections are available only electronically resolved and only for a few transitions also vibrationally resolved cross sections exist [12]. As a result, rotational excitation is typically neglected in population models for  $H_2$ .

As already mentioned, new ro-vibrationally resolved corona models for the Werner band and the Lyman band have been developed. These models use transition probabilities and excitation cross sections specifically calculated for this purpose, as described in the following section. Due to the continuous character of the  $a^3 \rightarrow b^3$  band, the vibrationally resolved model used in [3] is sufficient

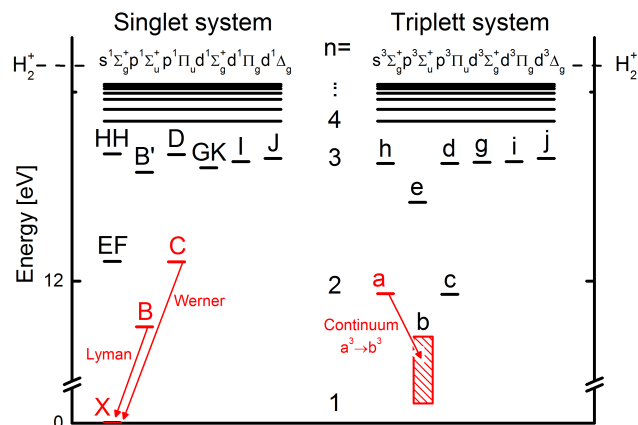


Figure 1: Energy level diagram showing the lowest electronic states of  $H_2$ . Indicated in red are the Werner and Lyman bands and the continuum  $a^3 \rightarrow b^3$ .

for describing the spectral distribution of the photons emitted by this transition. All three transitions under investigation are indicated in red in Figure 1.

### 3.2. Extension of the data base

Used as input for extending the available data set for  $H_2$  population models have been potential energy curves (i.e. the eigenvalues of the electronic part of the molecular wave functions) for the electronic states  $X^1$ ,  $B^1$  and  $C^1$  from [13]. Additionally, the adiabatic correction terms from [13] for  $H_2$  have been applied to the potential curves. Within the Born Oppenheimer approximation vibration and rotation of the molecule are independent of the electronic excitation and the ro-vibrational eigenvalues and eigenfunctions can be determined by solving the Schrödinger equation for the potential well described by the potential energy curves. This has been done by applying the computer code Level[14].

In a second step the ro-vibrational eigenfunctions have been used in order to calculate ro-vibrationally resolved Franck Condon factors and – in combination with the appropriate electronic dipole transition moments[13] and Hönl London factors[15] – transition probabilities for the Werner and Lyman band transitions. While preparing these data it was taken into account that due to the different possible combinations of the nuclear spins two different modifications of  $H_2$  exist: ortho-hydrogen (statistical weight: 3) and para-hydrogen (statistical weight: 1). Depending on the angular momentum of the electrons rotational levels exist solely in one of the two modifications or in both of them. Under normal circumstances transitions between ortho- and para-hydrogen are impossible.

In order to check the accuracy of the obtained results the calculated eigenvalues and transition probabilities have been compared with data available in the literature[10,16]: for low rotational quantum numbers  $J$  the deviations of the eigenvalues are below one  $cm^{-1}$  but they increase to several  $cm^{-1}$  with increasing  $J$ . One possible reason for the latter observation is that the present calculations do not take into account the nonadiabatic correction of the potential curves and relativistic correction terms. The transition probabilities agree very well with the available literature values – with the exception of some ro-vibrational states that are perturbed due to strong coupling with other states (e.g. close to avoided crossings of potential curves), an effect that is not taken into account by the present calculations.

Ro-vibrationally resolved electron collision excitation cross sections have been generated based on electronically resolved data from [17] and using the Gryzinski method [18].

### 4. Results

Figure 2 shows simulated spectra for the Werner and Lyman band and the continuum  $a^3 \rightarrow b^3$  in the hot driver plasma of the prototype negative ion source for ITER NBI. The following plasma parameters have been used as input for the calculations with the corona models and the CR model:  $T_e=10$  eV,  $n_e=5 \cdot 10^{18} m^{-3}$ ,  $n(H_2)=5 \cdot 10^{19} m^{-3}$ ,  $T_{rot}=850$  K and  $T_{vib}=5000$  K (the latter two temperatures hold for the ground state  $X^1$ ). It is assumed that due to the small energy gaps the rotational states thermalize and thus  $T_{rot}$  for the electronically excited states was determined by multiplying  $T_{rot}$  of the ground state with the respective ratio of the rotational constants  $B_e$ [15]. For the emitted lines a Gaussian structure has been used,  $\sigma=14$  pm (describing mainly the apparatus profile of the simulated detector). Additionally shown is the calculated  $a^3 \rightarrow b^3$  continuum emission from [2]. The amount of photons emitted by the Werner and Lyman bands ( $6.85 \cdot 10^{23}$  Ph/( $m^3 s$ )) is by a factor of two larger compared to the photons

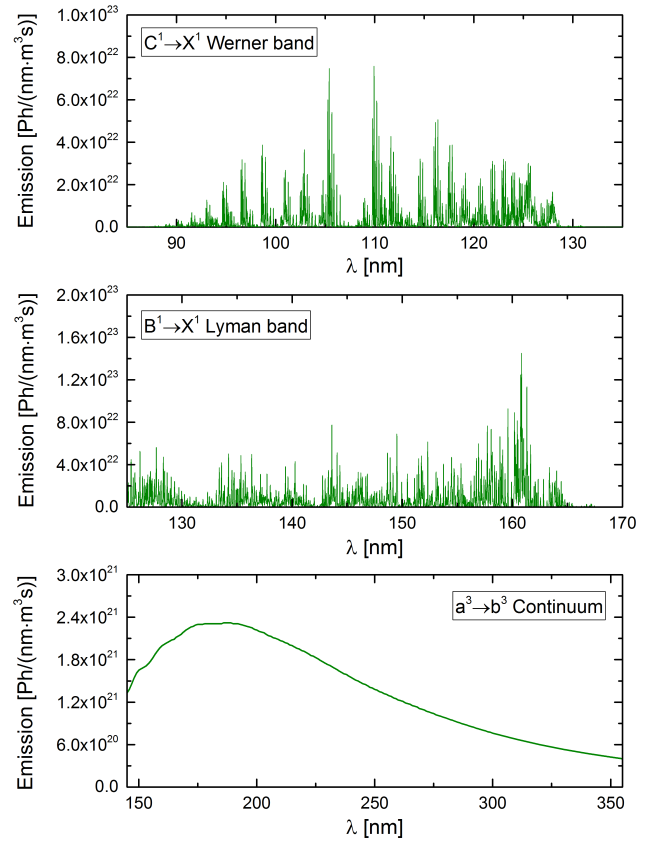


Figure 2: Simulated spectra for the Werner and Lyman band and for the continuum  $a^3 \rightarrow b^3$  in  $H_2$ .

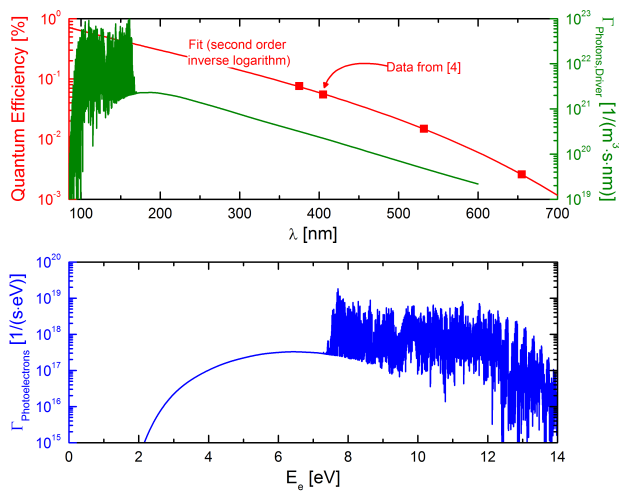


Figure 3: a) QE for a caesium covered tungsten surface. Flux density of UV photons generated in the driver. b) Rate of PE production at the PG surface.

originating from the continuum  $a^3 \rightarrow b^3$  ( $3.42 \cdot 10^{23}$  Ph/(m<sup>3</sup>s)).

Figure 3a shows the QE of a thick (more than one mono layer) caesium layer on W together with the photon flux density emitted in the driver. In order to determine the total photon flux, the flux density was multiplied with the volume of the driver ( $6.8 \cdot 10^{-3}$  m<sup>3</sup>). From the ratio of the inner driver surfaces it was estimated that about 22 % of these photons are able to leave the driver volume. The rate of PE production at the PG surface – calculated assuming that all photons leaving the driver hit the grid surface – is shown in Figure 3b.

For typical working conditions of the ion source the production rate of negative ions produced at the PG surface ( $5.51 \cdot 10^{21}$  1/(m<sup>2</sup>s)) is about 157 times larger than the one of PE ( $3.52 \cdot 10^{19}$  1/(m<sup>2</sup>s)). Additionally, due to the high mass ratio ( $m(H^-)/m_e \approx 1823$ ) the PE move significantly faster than the negative ions. Thus, their density in the plasma is small and only a small influence of the PE on the properties of the sheath and the plasma can be expected. The latter statement was proven by implementing the determined total PE flux into the Bacon code: the calculated shapes of the sheath with and without PE are virtually identical; the same holds for the particle densities in the bulk plasma and the flux of surface produced negative hydrogen ions towards the bulk plasma.

## 5. Conclusions

Ro-vibrationally resolved corona models for the Werner and Lyman band transitions in H<sub>2</sub> have been developed. These models are based on newly calculated transition probabilities and electron

collision excitation cross sections. In combination with existing vibrationally resolved model for the continuum  $a^3 \rightarrow b^3$  the flux of UV photons generated in the driver of the prototype negative ion source for ITER NBI was calculated and the resulting flux of PE generated on the PG surface was deduced. Using the 1d3v PIC code Bacon it was shown that the main conclusion made in [3] is still valid when besides the H<sub>2</sub> continuum  $a^3 \rightarrow b^3$  the Werner and the Lyman bands are taken into account: the PE do not significantly influence the plasma sheath, the properties of the bulk plasma and the flux of negative hydrogen ions towards the bulk plasma.

## 6. Acknowledgements

The first author wishes to thank Professor Kurt Behringer for useful discussions on simulating the emission bands of H<sub>2</sub> and Janne Laulainen for comments on the QE of caesiated surfaces.

## 7. References

- [1] P. Franzen et al, Nucl. Fusion **47** (2007) 264
- [2] V. Dudnikov, Rev. Sci. Instrum. **73** (2002) 992
- [3] D. Wunderlich et al, *Proceedings 30th ICPIG*, 2011
- [4] K. L. Jensen et al, J. Appl. Phys **102** (2007) 074902
- [5] D. Wunderlich et al, Plasma Sources Sci. Technol. **18** (2009) 045031
- [6] D. Wunderlich et al, J. Quant. Spectrosc. Radiat. Transfer **110** (2009) 62
- [7] K. Sawada et al, J. Appl. Phys. **78** (1995) 2913
- [8] <http://adas.phys.strath.ac.uk>
- [9] U. Fantz et al, At. Data Nucl. Data Tables **92** (2006) 853
- [10] H. Abgrall et al, J. Molec. Spectr. **157** (1993) 512
- [11] S. A. Astashkevich et al, J. Quant. Spectrosc. Radiat. Transfer **56** (1996) 725
- [12] R. Celiberto et al, At. Data Nucl. Data Tables **77** (2001) 161
- [13] [fizyka.umk.pl/ftp/pub/publications/ifiz/luwo/](http://fizyka.umk.pl/ftp/pub/publications/ifiz/luwo/)
- [14] <http://leroy.uwaterloo.ca/programs/>
- [15] G. Herzberg, *Molecular Spectra and Molecular Structure, I. Spectra of Diatomic Molecules*, Van Nostrand 1950
- [16] H. Abgrall et al, Astronom. Astrophys. Suppl. Ser. **141** (2000) 297
- [17] W.T. Miles et al, J. Appl. Phys. **43** (1972) 678
- [18] M. Gryzinski, Phys. Rev. **138** (1965) A336